Rashba-effect-induced spin dephasing in n-type InAs quantum wells

2003 J. Phys.: Condens. Matter 15 5563

(http://iopscience.iop.org/0953-8984/15/32/316)

INSTITUTE OF PHYSICS PUBLISHING JOURNAL OF PHYSICS: CONDENSED MATTER

J. Phys.: Condens. Matter **15** (2003) 5563–5576 PII: S0953-8984(03)64177-9

Rashba-effect-induced spin dephasing in n-type InAs quantum wells

M Q Weng and M W Wu[1]

Structure Research Laboratory, University of Science and Technology of China, Academia Sinica, Hefei, Anhui 230026, People's Republic of China
and
Department of Physics, University of Science and Technology of China, Hefei, Anhui 230026, People's Republic of China

E-mail: mwwu@ustc.edu.cn

Received 28 May 2003
Published 1 August 2003
Online at stacks.iop.org/JPhysCM/15/5563

Abstract

We perform a many-body investigation of the spin dephasing in n-type InAs quantum wells under moderate magnetic fields in the Voigt configuration by constructing and solving numerically the kinetic Bloch equations. We obtain the spin dephasing time due to the Rashba effect together with the spin-conserving scattering such as electron–phonon, electron–nonmagnetic impurity as well as electron–electron Coulomb scattering. By varying the initial spin polarization, temperature, impurity density, applied magnetic field and the interface electric field, we are able to study the spin dephasing time under various conditions. For the electron density and quantum well width that we study, the many-body effect dominates the spin dephasing. Moreover, we find an anomalous resonance peak in the spin dephasing time for high initial spin polarization under moderate magnetic fields.

1. Introduction

Almost all of the current semiconductor devices are based on manipulating electronic charges. The upcoming field of spintronics proposes using the spin degree of freedom of electrons in place of (or in addition to) the charge degree of freedom for device applications in order to add new features and functionalities to semiconductors devices [1–3]. The prospects for realizing the proposed spintronic devices are supported by the recent development of ultra-fast nonlinear optical experiments [4–17] where long spin dephasing time (>100 ns) is reported.

The functionalities of semiconductor spintronic devices rely on the manipulation of the spin coherence. To realize these devices, one needs to understand thoroughly the spin

[1] Address for correspondence: Department of Physics, University of Science and Technology of China, Hefei, Anhui 230026, People's Republic of China.

0953-8984/03/325563+14$30.00

dephasing mechanisms that tend to destroy the spin coherence. Historically, three spin dephasing mechanisms have been proposed in semiconductors [18–20]: the Elliot–Yafet (EY) mechanism [21, 22], the D'yakonov–Perel' (DP) mechanism [23], and the Bir–Aronov–Pikus (BAP) mechanism [24]. All three mechanisms are either due to the spin flip (SF) scattering or treated as effective SF scattering. The spin dephasing times of these mechanisms for a low polarized system are calculated in the framework of single-particle approximation [18]. In additional to these single-particle spin dephasing mechanisms, three years ago Wu proposed a many-body spin dephasing mechanism which has long been overlooked in the literature. This mechanism is caused by irreversibly disrupting the phases between spin dipoles due to inhomogeneous broadening together with spin-conserving (SC) scattering [25–29]. It is therefore a many-body effect. The inhomogeneous broadening can be introduced through the energy dependence of g-factor [25, 29, 30] and/or the momentum $\boldsymbol{k}$-dependence of the DP term [26, 27, 29]. Our recent work shows further that this mechanism also plays an important role in the spin dephasing during spin transport [31, 32].

Very recently we performed a systematic investigation [33, 34] of the spin dephasing due to the DP effect in n-typed GaAs (100) quantum wells (QWs) for high temperatures ($\geqslant$120 K) under magnetic fields in the Voigt configuration by constructing and solving numerically the kinetic Bloch equations [25–29, 35]. In these studies, we include all SC scattering, such as the electron–phonon, electron–nonmagnetic impurity and electron–electron Coulomb scattering, and investigate the spin dephasing under various conditions. The dephasing obtained from our theory contains both the single-particle dephasing caused by the effective SF scattering first proposed by D'yakonov and Perel' [23] as well as the many-body dephasing due to the inhomogeneous broadening provided by the DP term. We show that, for the electron densities we studied, the spin dephasing rate is dominated by the many-body effect. Moreover, as we include the electron–electron Coulomb scattering, we are able to investigate the spin dephasing with extra-large spin polarization (up to 100%) which has not been discussed either theoretically or experimentally. We find that, under moderate magnetic fields, the SDT increases dramatically with the initial spin polarization. For example, the SDT of an impurity-free sample gets an increase of more than one order of magnitude when the initial spin polarization rises from about 0 to about 100% at low temperature [33]. The initial-spin-polarization dependence of the spin dephasing becomes more interesting when the magnetic field is increased to a few tens of tesla, where the SDT no longer increases monotonically with the initial spin polarization but shows an anomalous resonance peak versus the initial spin polarization [34]. The dramatic increase and the anomalous resonance of SDT in the high-spin-polarization region is found to be due to the first order of the electron–electron interaction, i.e. the Hartree–Fock (HF) contribution, which provides an effective magnetic field that can reduce the spin dephasing and result in a fast increase in the SDT. Moreover, under the right condition, the HF term, the applied magnetic field and the DP term can reach a resonance, and thus form the anomalous peak. Due to the small Landé g-factor in GaAs, the resonance condition can only be achieved under very high magnetic fields.

In this paper, we apply kinetic theory to study the spin dephasing in the n-type InAs QW for high temperatures where the DP term is the leading dephasing mechanism. In the QW system, the DP term is composed of the Dresselhaus term [36] and the Rashba term [37, 38]. The Dresselhaus term is due to the lack of inversion symmetry in the zinc-blende crystal Brillouin zone and is sometimes referred to as the bulk inversion asymmetry (BIA) term. The Rashba term appears if the self-consistent potential within a QW is asymmetric along the growth direction and is therefore referred to as the structure inversion asymmetry (SIA) contribution. For QWs composed of wide band-gap semiconductors such as GaAs the Dresselhaus term is the main spin dephasing mechanism, whereas for QWs of narrow band-gap semiconductors

such as InAs (as in the present case) the Rashba term is dominant. As the Rashba term is proportional to the interface electric field of the QW, the spin dephasing in the InAs QW can be manipulated through applying an electric field perpendicular to the QW. Moreover, as the Landè g-factor in InAs is very large ($g = 15$ compared to 0.44 of GaAs), one expects the resonance condition to be achieved under a moderate magnetic field. The paper is organized as follows. We present our model and the kinetic equations in section 2. Then, in section 3.1, we investigate how the SDT changes with the variation in the initial spin polarization. The temperature dependence of the SDT under different spin polarizations is discussed in detail in section 3.2, where we also highlight the difference between the present many-body theory and the earlier simplified theory. In section 3.3 we show the magnetic field dependence of the SDT. Finally, we discuss how the interface electric field affects the SDT. We present the conclusion and summary in section 4.

2. Kinetic equations

We start our investigation from an n-doped (100) InAs QW with a well width of a. The growth direction is assumed to be along the z-axis. A moderate magnetic field $\boldsymbol{B}$ is applied along the x-axis. Due to the confinement of the QW, the momentum states along the z-axis are quantized. Therefore, the electron states are characterized by a sub-band index n and a two-dimensional wavevector $\boldsymbol{k} = (k_x, k_y)$ together with a spin index σ. In this paper we choose the electron density so that only the lowest sub-band is populated and the transition to the upper sub-bands is unimportant. Therefore, one only needs to consider the lowest sub-band. With the DP term (specifically the Rashba term) included, the Hamiltonian of the electrons in the QW takes the form

$$H = \sum_{\boldsymbol{k}\sigma\sigma'} \left\{ \varepsilon_{\boldsymbol{k}} + [g\mu_{\mathrm{B}}\boldsymbol{B} + \boldsymbol{h}(\boldsymbol{k})] \cdot \frac{\vec{\boldsymbol{\sigma}}_{\sigma\sigma'}}{2} \right\} c^{\dagger}_{\boldsymbol{k}\sigma} c_{\boldsymbol{k}\sigma'} + H_{\mathrm{I}}. \tag{1}$$

Here $\varepsilon_{\boldsymbol{k}} = \boldsymbol{k}^2/2m^*$ is the energy of an electron with wavevector $\boldsymbol{k}$ and effective mass m^*, and $\vec{\boldsymbol{\sigma}}$ are the Pauli matrices. The Rashba term $\boldsymbol{h}(\boldsymbol{k})$ can be written as

$$h_x(\boldsymbol{k}) = \alpha k_y, \qquad h_y(\boldsymbol{k}) = -\alpha k_x, \qquad h_z(\boldsymbol{k}) = 0. \tag{2}$$

In these equations, α is proportional to the interface electric field E_z along the growth direction:

$$\alpha = \alpha_0 e E_z, \tag{3}$$

where the coefficient α_0 is inversely proportional to the energy gap and the effective mass [39]. The interaction Hamiltonian H_{I} is composed of Coulomb interaction H_{ee}, electron–phonon interaction H_{ph}, as well as electron–impurity scattering H_{i}. Their expressions can be found in textbooks [40, 41].

We construct the kinetic Bloch equations by using the nonequilibrium Green function method [40] as follows:

$$\dot{\rho}_{\boldsymbol{k},\sigma\sigma'} = \dot{\rho}_{\boldsymbol{k},\sigma\sigma'}|_{\mathrm{coh}} + \dot{\rho}_{\boldsymbol{k},\sigma\sigma'}|_{\mathrm{scatt}}. \tag{4}$$

Here $\rho_{\boldsymbol{k}}$ represents the single-particle density matrix. The diagonal elements describe the electron distribution functions $\rho_{\boldsymbol{k},\sigma\sigma} = f_{\boldsymbol{k}\sigma}$. The off-diagonal elements $\rho_{\boldsymbol{k},\frac{1}{2}-\frac{1}{2}} \equiv \rho_{\boldsymbol{k}}$ describe the inter-spin-band polarizations (coherence) of the spin coherence [35]. Note that $\rho_{\boldsymbol{k},-\frac{1}{2}\frac{1}{2}} \equiv \rho^*_{\boldsymbol{k},\frac{1}{2}-\frac{1}{2}} = \rho^*_{\boldsymbol{k}}$. Therefore, $f_{\boldsymbol{k}\pm\frac{1}{2}}$ and $\rho_{\boldsymbol{k}}$ are the quantities to be determined from the Bloch equations.

The coherent part of the equation of motion for the electron distribution function and the spin coherence are given by

$$\left.\frac{\partial f_{\boldsymbol{k},\sigma}}{\partial t}\right|_{\rm coh} = -2\sigma\{[g\mu_{\rm B}B + h_x(\boldsymbol{k})]\,{\rm Im}\,\rho_{\boldsymbol{k}} + h_y(\boldsymbol{k})\,{\rm Re}\,\rho_{\boldsymbol{k}}\} + 4\sigma\,{\rm Im}\sum_q V_q\rho^*_{\boldsymbol{k}+q}\rho_{\boldsymbol{k}}, \tag{5}$$

$$\left.\frac{\partial \rho_{\boldsymbol{k}}}{\partial t}\right|_{\rm coh} = \frac{1}{2}[{\rm i}g\mu_{\rm B}B + {\rm i}h_x(\boldsymbol{k}) + h_y(\boldsymbol{k})](f_{\boldsymbol{k}\frac{1}{2}} - f_{\boldsymbol{k}-\frac{1}{2}}) + {\rm i}\sum_q V_q[(f_{\boldsymbol{k}+q\frac{1}{2}} - f_{\boldsymbol{k}+q-\frac{1}{2}})\rho_{\boldsymbol{k}} - \rho_{\boldsymbol{k}+q}(f_{\boldsymbol{k}\frac{1}{2}} - f_{\boldsymbol{k}-\frac{1}{2}})], \tag{6}$$

respectively, where $V_q = 2\pi e^2/[\kappa_0(q+q_0)]$ is the 2D Coulomb matrix element under static screening, $q_0 = (e^2m^*/\kappa_0)\sum_\sigma f_{k=0,\sigma}$, and κ_0 is the static dielectric constant. The first term on the right-hand side (rhs) of equation (5) describes the spin precession of electrons under the magnetic field $\boldsymbol{B}$ as well as the effective magnetic field $\boldsymbol{h}(\boldsymbol{k})$ due to the Rashba effect. The scattering terms of the electron distribution function and the spin coherence are given by equations (A.1) and (A.2) in the appendix.

The initial conditions, at $t = 0$, are taken as

$$\rho_{\boldsymbol{k}}|_{t=0} = 0, \tag{7}$$

$$f_{\boldsymbol{k}\sigma}|_{t=0} = 1/\{\exp[(\varepsilon_{\boldsymbol{k}} - \mu_\sigma)/k_{\rm B}T] + 1\}, \tag{8}$$

where μ_σ is the chemical potential for spin σ. The condition $\mu_{\frac{1}{2}} \neq \mu_{-\frac{1}{2}}$ gives rise to the imbalance of the electron densities of the two spin bands.

3. Numerical results

The kinetic Bloch equations form a set of nonlinear equations. All the unknowns to be solved appear in the scattering terms. Specifically, the electron distribution function is no longer a Fermi distribution because of the existence of the anisotropic Rashba term $\boldsymbol{h}(\boldsymbol{k})$. This term in the coherent part drives the electron distribution away from an isotropic Fermi distribution. The scattering term attempts to randomize electrons in $\boldsymbol{k}$-space. Obviously, both the coherent part and the scattering terms must be solved self-consistently to obtain the distribution function and the spin coherence.

We solve numerically the kinetic Bloch equations in a self-consistent fashion in order to study the spin precession between the spin-up and spin-down bands. We include electron–phonon scattering and the electron–electron interaction throughout our computation. As we concentrate on the relatively high-temperature regime in this study, for electron–phonon scattering we only need to include electron–LO phonon scattering. Electron–impurity scattering is sometimes excluded. As discussed in the previous paper [35, 42], irreversible spin dephasing time can be defined well by the inverse of the slope of the envelope of the incoherently summed spin coherence $\rho(t) = \sum_{\boldsymbol{k}} |\rho_{\boldsymbol{k}}|$. It is known that there are two time parameters for characterizing the spin relaxation. One is the longitudinal relaxation time T_1, which determines the recovery speed of the longitudinal magnetization and hence characterizes the decay of the imbalance in the diagonal term of the density matrix. This time is generally referred to as the spin relaxation time. The other is the transverse relaxation time T_2, which describes the vanishing rate of the transverse spin momentum and therefore specifies the reduction in the off-diagonal term of the density matrix [43]. The irreversible transverse spin relaxation is called spin dephasing. Therefore the SDT obtained from our theory, which describes the irreversible reduction in the spin coherence, is just the irreversible transverse relaxation time T_2. The material parameters of InAs for our calculation are tabulated in

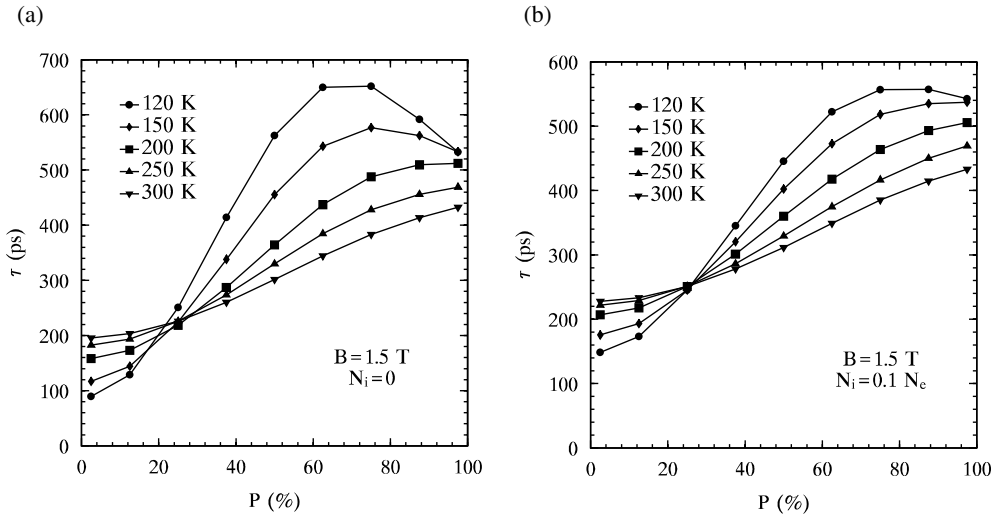

Figure 1. The spin dephasing time τ versus the initial spin polarization P for different impurity concentrations and temperatures. The impurity densities in (a) and (b) are 0 and $0.1N_e$, respectively. The curves are plotted as a visual aid.

Table 1. The parameters used in the numerical calculations.

κ_∞	12.25	κ_0	15.15
ω_0	27 meV	m^*	$0.0239\ m_0$
a	7.5 nm		

table 1 [44]. The numerical calculation method has been laid out in detail in the previous paper on the DP mechanism in 3D systems [25]. The difference is that here we are able to obtain the results quantitatively instead of only qualitatively, as in the previous 3D case, due to the smaller dimension in momentum space. Our main results are plotted in figures 1–6. In these calculations the total electron density N_e and the applied magnetic field B are chose to be 4×10^{10} cm^{-2} and 1.5 T, respectively, unless otherwise specified.

3.1. Spin polarization dependence of the spin dephasing time

We first study the spin polarization dependence of the SDT. Since our theory is a many-body theory and we include all the scattering (especially the Coulomb scattering) in our calculation, we are able to calculate the SDT with large spin polarization.

In figure 1, SDT (τ) is plotted against the initial spin polarization P for $N_i = 0$ (a) and $N_i = 0.1N_e$ (b) at different temperatures. The most striking feature of the impurity-free case is the huge anomalous peaks in SDT at low temperatures. For $T = 120$ K, the peak value of the SDT is about six times higher than that for low initial spin polarization. It is also seen from the figure that the anomalous peak is reduced with an increase in temperature and that the peak shifts to higher polarization. For $T > 200$ K there is no anomalous peak.

The anomalous peak in the τ–P curve in the low-temperature region originates from the electron–electron interaction, specifically the HF self-energy (i.e. the last terms in equations (5) and (6)). If one removes the HF term, then the anomalous peak and the large increase in SDT disappear. In our previous paper, it was pointed out that, although the HF term itself does not

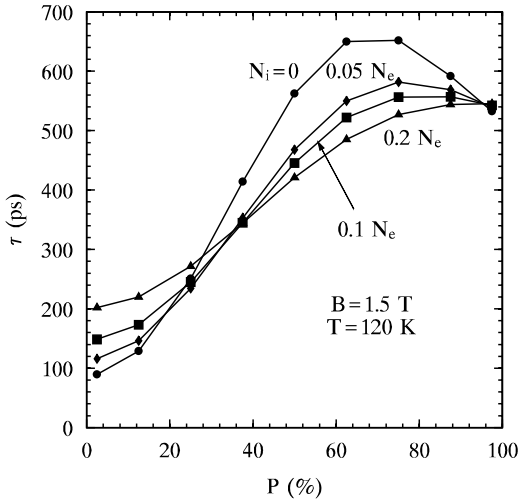

Figure 2. The spin dephasing time τ versus the initial spin polarization P for an InAs QW with different impurity levels: circle (●), $N_i = 0$; diamond (♦), $N_i = 0.05N_e$; square (■), $N_i = 0.1N_e$; triangle (▲), $N_i = 0.2N_e$. The curves are plotted as a visual aid.

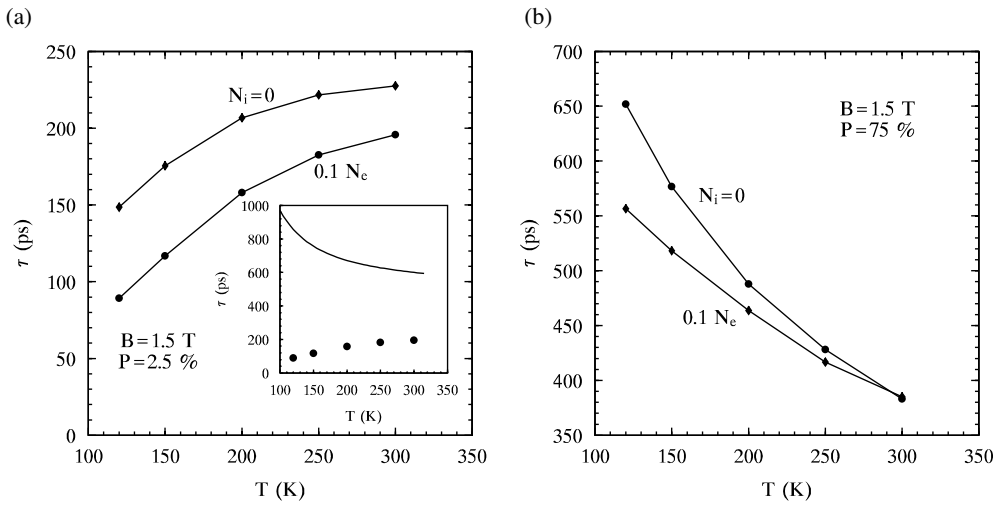

Figure 3. The spin dephasing time τ versus temperature T for InAs QWs with spin polarization $P = 2.5\%$ (a) and $P = 75\%$ (b) for two different impurity levels: circle (●), $N_i = 0$; diamond (♦), $N_i = 0.1N_e$. The curves are plotted as a visual aid. The SDT predicted by the simplified treatment of the Rashba term (solid curve) and our model (circle) for $N_i = 0$ are plotted in the inset of (a) for comparison.

contribute directly to the spin dephasing [28, 29], it can affect the motion of the electrons as it behaves as an effective magnetic field $\boldsymbol{B}^{\mathrm{HF}}(\boldsymbol{k})$. Therefore, the HF term can affect the spin dephasing by combining with the Rashba term. For small spin polarization, as is commonly discussed in the literature, the contribution of the HF term is marginal. However, when the polarization increases, then the HF contribution becomes larger. In particular, the effective magnetic field formed by the HF term contains a longitudinal component $[B_z^{\mathrm{HF}}(\boldsymbol{k})]$ which can

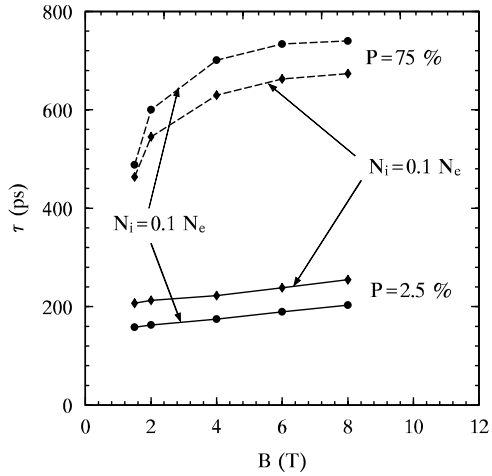

Figure 4. The spin dephasing time τ versus the applied magnetic field for InAs QWs for different spin polarizations and impurity levels: solid line with dots, $N_{\rm i} = 0$, $P = 2.5\%$; solid curve with diamonds, $N_{\rm i} = 0.1N_{\rm e}$, $P = 2.5\%$; dashed curve with dots, $N_{\rm i} = 0$, $P = 75\%$; dashed curve with diamonds, $N_{\rm i} = 0.1N_{\rm e}$, $P = 75\%$.

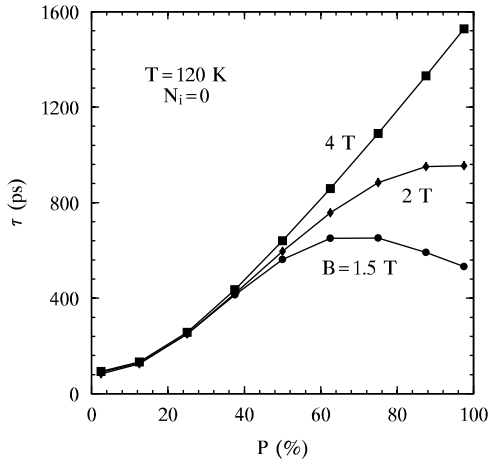

Figure 5. The spin dephasing time τ versus polarization for InAs QWs at different magnetic fields: circle (●), $B = 1.5$ T; diamond (♦), $B = 2$ T; square (■), $B = 4$ T. The lines are plotted as a visual aid.

effectively reduce the 'detuning' of the spin-up and spin-down electrons and thus strongly reduce the spin dephasing, so the SDT increases with initial spin polarization [33]. Moreover, besides the initial polarization, ρ_k and therefore $B^{\rm HF}(k)$ are also affected by the applied magnetic field. With higher magnetic field, both become larger. Under a high magnetic field and when the initial spin polarization reaches the right value, the effective magnetic field $B^{\rm HF}(k)$ may reach a magnitude comparable to the contribution from the Rashba term, as well as the applied magnetic field in the coherent parts of the Bloch equations, and reduce the anisotropy caused by the Rashba term. Therefore, one obtains a much longer SDT. However, if one further increases the initial polarization, then the HF term exceeds the resonance condition. As a result, the SDT decreases. Therefore, one obtains the anomalous peak, which is similar

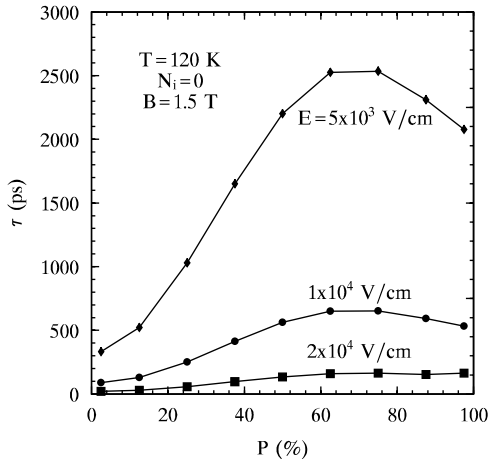

Figure 6. The spin dephasing time τ versus the initial spin polarization at $T = 120$ K, $B = 1.5$ T and $N_i = 0$ for three different interface electric fields.

to the resonance effect. It is noted that, as both the DP and HF terms are k-dependent, the resonance is broadened.

For high temperatures the HF term is smaller. In order to reach resonance, one needs to go to higher polarization. Therefore, as shown in the figure, the anomalous peak shifts to higher polarization. However, when the temperature is high enough, even the largest polarization ($P = 100\%$) cannot make the HF term reach the resonance condition. Therefore, the peak disappears.

The τ–P curve is much different when the impurities are introduced. It is seen from figure 1(b) that, when the impurity density is large (say $N_i = 0.1N_e$), the fast rise in the τ–P curve remains. Nevertheless, the increase is smaller than the corresponding increase when impurities are absent. As well as the reduction in the rise in the τ–P curves, the impurities destroy the anomaly too. One can easily see that, with impurity level $N_i = 0.1N_e$, when the temperature is 120 K then the anomalous peak is much flatter than the impurity-free sample while, for all other temperatures we study, the SDT increases uniquely with polarization.

To reveal further the contribution of the impurity to the dephasing under different conditions, in figure 2 we plot the SDT as a function of polarization for different impurity levels at $T = 120$ K. The figure clearly shows that the impurity tends to remove the anomalous peak and shift the peak to the larger initial spin polarization. This is because the impurity reduces the HF term, and therefore the resonance effect is also reduced. Hence, in order to reach the maximum resonance, one has to increase the initial spin polarization. Consequently, the peak shifts to larger P. However, when N_i is raised to $0.2N_e$, the HF term is reduced too much to form a peak.

3.2. The temperature dependence of the spin dephasing time

In the above we discussed the dependence of spin dephasing on initial spin polarization for different temperatures. Now we turn to the temperature dependence of the SDT under different initial spin polarizations. From figures 1(a) and (b) in section 3.2 one can see that, for small polarization, the SDT increases with temperature. In contrast, in the highly polarized region the SDT decreases with the temperature. For moderate polarization, the temperature dependence is too complicated to be described by a monotonic function of temperature.

To see more detail of how the spin dephasing depends on temperature, in figures 3(a) and (b) we re-plot the SDT shown in figure 1 as a function of temperature for different impurity levels and spin polarizations. It is seen from the figure that, similarly to the case for GaAs where the DP term is composed of the Dresselhaus term [33], for the Rashba term and for low spin polarization the SDT also increases with temperature for all impurity levels. This property is again *opposite* to the results of earlier simplified treatments of the DP effect, where it was predicted that the spin lifetime decreases with an increase in temperature in the 2D system [45, 46]. The SDT, based on the simplified model, is given by [27, 45, 47]

$$\frac{1}{\tau} = \frac{\int_0^\infty \mathrm{d}E_k (f_{k\frac{1}{2}} - f_{k-\frac{1}{2}})\Gamma(k)}{\int_0^\infty \mathrm{d}E_k (f_{k\frac{1}{2}} - f_{k-\frac{1}{2}})}, \tag{9}$$

in which

$$\Gamma(k) = 2\tau_1(k)(\alpha_0 E k)^2 \tag{10}$$

and

$$\tau_n^{-1}(k) = \int_0^{2\pi} \sigma(E_k, \theta)[1 - \cos(n\theta)]\,\mathrm{d}\theta. \tag{11}$$

Here, $\sigma(E_k, \theta)$ represents the scattering cross-section. For comparison, in the inset of figure 3(a) we plot the SDT predicted by the earlier model and by our present many-body theory. From the inset, one can see that the SDT predicted by the earlier model is about one order of magnitude larger than that predicted by our theory. In the meantime, the SDT of the earlier mode drops dramatically with an increase in temperature. Nevertheless, in our many-body treatment it rises slightly with temperature.

The huge difference between the two models lies in the fact that the earlier simplified model is based on the single-particle picture. This does not account for the dephasing due to the inhomogeneous broadening inherited in the Rashba term, which is exactly the result of the many-body effect [25–29]. By comparing the theoretical SDT predicted by the two models, we can see that the spin dephasing due to the inhomogeneous broadening is much more important. In the case that we calculated, the spin dephasing is dominated by the inhomogeneous broadening. Therefore, it is easy to understand why the earlier simplified treatment of the DP mechanism gives much slower spin dephasing. Although there is no experimental results for InAs, we have shown that for GaAs the prediction of our many-body theory agrees both quantitatively and qualitatively with the experimental results [33].

The temperature dependence of the SDT can be understood easily when the spin dephasing due to inhomogeneous broadening is taken into account: when the temperature increases, the inhomogeneous broadening is reduced as the electrons are distributed to the wider $\boldsymbol{k}$-states. As a result, the number of electron occupations on each $\boldsymbol{k}$-state is reduced. It is further noted that this reduction is a mild function of temperature. Therefore, the temperature dependence is quite mild unless it is within the regime of the anomalous peak.

In the region where the HF term is important, in addition to the above-mentioned two effects of the temperature acting on the spin dephasing, the temperature dependence of the HF term should also be taken into account when we study the temperature dependence of the spin dephasing. In the high-spin-polarization region, the SDT decreases with temperature. However, in the moderately polarized region, the temperature dependence of SDT due to the combination of these three effects is too complicated to be described by a monotonic function. In figure 3(b) we re-plot the SDT as a function of temperature for high polarization ($P = 75\%$), which is near to the anomalous peak shown in figure 1(a). We can see that, due to the reduction in the HF term, the resonance is removed and the SDT drops dramatically

with the increase in temperature in the impurity-free sample. Meanwhile, for the system with impurity concentration $N_i = 0.1N_e$, the HF term is less important than that in the impurity-free sample and the SDT is less sensitive to temperature.

3.3. Magnetic field dependence of the spin dephasing

We now investigate the magnetic field dependence of the spin dephasing. In figure 4 we plot the SDT versus the applied magnetic field for different impurity levels and spin polarizations. It is seen that, for all the cases we study, the SDT increases with magnetic field. This is because, in the presence of a magnetic field, the electron spins undergo a Larmor precession around the magnetic field. This precession suppresses the precession about the effective magnetic field $\boldsymbol{h}(\boldsymbol{k})$ [18, 30]. Therefore, the SDT increases with magnetic field. It is pointed out that, in a 3D electron gas, the magnetic field also forces electrons to precess around it. This precession introduces additional symmetry in the momentum space that limits the $\boldsymbol{k}$-space available to the DP effect, which is anisotropic in it [18, 25, 30]. This can further reduce the spin dephasing. However, it is expected that this effect in the 2D case is less effective than in the 3D case since, in the z-direction, the momentum is quantized and momentum precession around the magnetic field should be suppressed.

In addition to the above-mentioned effect of the magnetic field on spin dephasing, one can further see from figure 4 that, for large polarization, the magnetic field also enhances the HF term. As we mentioned before, for large polarization the contribution from the HF term is important. An increase in the HF term serves as an additional magnetic field that further suppresses the effect of the Rashba term $\boldsymbol{h}(\boldsymbol{k})$ and therefore results in a faster rise in the τ–B curve in the region of $B < 4$ T. When the applied magnetic field exceeds 4 T, the increase in the HF term saturates, thus the slope of the τ–B curves in the region of $B > 4$ T is reduced to that in the low-polarization region. To reveal more about the combined effect of the magnetic field and the HF term on spin dephasing, in figure 5 we plot SDT as a function of polarization. It is shown that the rise in the τ–P curve increases with magnetic field. Moreover, the position of the peak in the τ–P curve shifts to larger polarization. It is understood that this needs a larger HF term, and hence a larger spin polarization, to achieve the resonance condition when the magnetic field increases. When the magnetic field is raised to 4 T, it is no longer possible to form the resonance for all of the polarization. As a result, the SDT increases uniquely with polarization and there is no peak in the τ–P curve.

3.4. Interface electric field dependence of spin dephasing

We now investigate how the interface electric field affects the spin dephasing. In figure 6 we plot the SDT as a function of the initial spin polarization for three different interface electric fields. It can be seen from the figure that, when the interface electric field decreases from 2×10^4 to 5×10^3 V cm^{-1}, the SDT increases about 16-fold. It is understood that, when the interface electric field increases, the Rashba effect is enhanced. Consequently, the spin dephasing is also enhanced. Moreover, for fixed initial spin polarization, the HF term is reduced when E_z is increased. As a result, the interface electric field E_z also changes the anomalous peak in the τ–P curve since, to achieve the resonance condition, one must go to higher polarization in order to get a large enough HF term. Consequently, the resonance peak is smoothed and the position moves to the higher initial spin polarization region when E_z increases, which is shown in figure 6.

4. Conclusion

In conclusion, we have performed a systematic investigation of the Rashba effect on the spin dephasing of n-type InAs QWs under moderate magnetic fields in the Voigt configuration. Based on the nonequilibrium Green function theory, we derived a set of kinetic Bloch equations for a two-spin-band model. This model includes electron–phonon and electron–impurity scattering as well as the electron–electron interaction. By solving numerically the kinetic Bloch equations, we study the time evolution of the electron densities in each spin band and the spin coherence, i.e. the correlation between the spin-up and spin-down bands. The spin dephasing time is calculated from the slope of the envelope of the incoherently summed spin coherence's time evolution. We are therefore able to study in detail how this dephasing time is affected by spin polarization, temperature, impurity level, magnetic field and interface electric field. In contrast to the earlier studies on spin dephasing that were based on the single-particle model (which considers only the effective SF scattering), our theory also takes account of the contribution of many-body effects on the spin dephasing [25–29]. In fact, for the n-type semiconductors and the spin polarization that were studied in the experiments, this many-body dephasing effect is even more important than the effective SF scattering, since it is one order of magnitude larger than the latter. Equally remarkable is the fact that, since we include in our many-body theory all scattering (in particular the Coulomb scattering), we are now able to calculate the spin dephasing with extra-large (up to 100%) initial spin polarization, which cannot be calculated using the previous single-particle theory.

It is found that the SDT increases with initial spin polarization. Moreover, for low impurity levels and low temperature, there is a huge anomalous resonant peak in the curve of SDT versus initial spin polarization. If one increases the impurity density, the temperature and/or the interface electric field (the magnetic field), then this resonant peak moves to high spin polarization and its magnitude is rapidly reduced (enhanced) until the whole resonance disappears. It is found that this anomalous resonance peak originates from the HF contribution of the electron–electron Coulomb interaction. Under the right spin polarization, the contribution of HF term may reach a magnitude comparable to the contribution of the Rashba term, as well as the magnetic field in the coherent part of the Bloch equation, and reduce the anisotropy caused by the Rashba effect—and consequently reduce the spin dephasing. As the resonance represents the combined effect of the HF term, the Rashba term and the magnetic field, the magnitude and position of the resonance peak are affected by all the factors that can affect the magnitude of the HF term, such as temperature, impurity scattering, magnetic field and the interface electric field: for a given impurity concentration, when the temperature increases, the HF term reduces. Consequently, the τ–P curve is smoothed and the peak position is moved to higher spin polarization. For the impurity-free sample, if the temperature is raised to 200 K, then the HF term is reduced too much to form a resonance and the anomalous peak disappears. The same situation occurs when the impurity level increases at a given temperature as the scattering also lowers the HF term. When the impurity level is raised to $0.2N_e$, there is no resonance in the temperature region we studied. Meanwhile, an increase in the magnetic field enhances the HF term and results in a faster increase in SDT as well as a higher resonant peak in the τ–P curve. Moreover, as the magnetic field increases, it needs a larger HF term and hence a larger polarization in order to achieve the resonance condition. Therefore the peak position is also moved to higher polarization. When the interface electric field increases, the HF term is reduced. Therefore the resonance peak in τ–P becomes flatter and its position moves to higher spin polarization.

For the low-spin-polarized regime, the SDT increases when the temperature rises. This is contrary to the result of earlier simplified single-particle calculations, where the SDT always

decreased with an increase in temperature. Moreover, the SDT predicted by our many-body calculation is one order of magnitude faster than the earlier result. The physics of this feature is due to the additional many-body spin dephasing channel that is due, in turn, to the inhomogeneous broadening provided by the Rashba term which, by combining with SC scattering, also causes spin dephasing. In the situation that we studied, spin dephasing is dominated by the many-body dephasing effect. With an increase in temperature, the inhomogeneous broadening reduces and the SDT increases.

In the high-spin-polarization region, the contribution of the HF term should be taken into consideration. This introduces more complexity into the study of spin dephasing. Usually, the SDT cannot be described by a monotonic function of temperature and impurity concentration in the high-polarization regime. For polarization near the resonance peak at low temperatures in impurity-free samples, the SDT decreases dramatically with temperature as the resonance is removed when the temperature increases. In contrast, when the impurity concentration is $0.1N_e$, the SDT is less sensitive to the temperature.

As the magnetic field causes the electron spins to precess about it, this precession will suppress the precession about the effective magnetic field $\boldsymbol{h}(\boldsymbol{k})$ that originates from the Rashba effect. As a result, the spin dephasing is reduced. The magnetic field also enhances the HF term, which serves as an additional magnetic field and further suppresses the Rashba effect. Therefore, the τ–B curve increases more quickly in the high-polarization region. Our calculation also shows that, when the interface electric field increases, the SDT decreases. This is because, with an increase in the interface electric field, the Rashba term is strengthened.

In summary, we have performed a thorough investigation of the spin dephasing in n-type InAs QWs. Many new features which have not previously been investigated either theoretically or experimentally are predicted over a wide range of parameters.

Acknowledgments

MWW is supported by the '100 Person Project' of the Chinese Academy of Sciences and the Natural Science Foundation of China under grant no 10247002. He would also like to thank S T Chui at Bartol Research Institute, University of Delaware for hospitality.

Appendix

The scattering terms of electron distribution functions in the Markovian limit are given by

$$\begin{aligned}\left.\frac{\partial f_{k,\sigma}}{\partial t}\right|_{\text{scatt}} = \Bigg\{ & -2\pi \sum_{qq_z\lambda} g^2_{qq_z\lambda}\delta(\varepsilon_k - \varepsilon_{k-q} - \Omega_{qq_z\lambda})[N_{qq_z\lambda}(f_{k\sigma} - f_{k-q\sigma}) + f_{k\sigma}(1 - f_{k-q\sigma}) \\ & - \operatorname{Re}(\rho_k \rho^*_{k-q})] - 2\pi N_i \sum_q U_q^2 \delta(\varepsilon_k - \varepsilon_{k-q})[f_{k\sigma}(1 - f_{k-q\sigma}) - \operatorname{Re}(\rho_k \rho^*_{k-q})] \\ & - 2\pi \sum_{qk'\sigma'} V_q^2 \delta(\varepsilon_{k-q} - \varepsilon_k + \varepsilon_{k'} - \varepsilon_{k'-q})[(1 - f_{k-q\sigma}) f_{k\sigma}(1 - f_{k'\sigma'}) f_{k'-q\sigma'} \\ & + \tfrac{1}{2}\rho_k \rho^*_{k-q}(f_{k'\sigma'} - f_{k'-q\sigma'}) + \tfrac{1}{2}\rho_{k'} \rho^*_{k'-q}(f_{k-q\sigma} - f_{k\sigma})] \Bigg\} \\ & - \{\boldsymbol{k} \leftrightarrow \boldsymbol{k} - \boldsymbol{q}, \boldsymbol{k}' \leftrightarrow \boldsymbol{k}' - \boldsymbol{q}\}, \end{aligned} \tag{A.1}$$

in which $\{\boldsymbol{k} \leftrightarrow \boldsymbol{k} - \boldsymbol{q}, \boldsymbol{k}' \leftrightarrow \boldsymbol{k}' - \boldsymbol{q}\}$ represents the same terms as in the previous brackets {} but with the interchange $\boldsymbol{k} \leftrightarrow \boldsymbol{k} - \boldsymbol{q}$ and $\boldsymbol{k}' \leftrightarrow \boldsymbol{k}' - \boldsymbol{q}$. The first term inside the braces on the rhs of equation (A.1) comes from the electron–phonon interaction. λ represents the

different phonon modes, i.e. one longitudinal optical (LO) phonon mode, one longitudinal acoustic (AC) phonon mode due to the deformation potential, and two AC modes due to the transverse piezoelectric field. $g_{qq_z\lambda}$ are the matrix elements of electron–phonon coupling for mode λ. For LO phonons, $g^2_{qq_z\mathrm{LO}} = \{4\pi\alpha\Omega^{3/2}_{\mathrm{LO}}/[\sqrt{2\mu}(q^2 + q_z^2)]\}|I(\mathrm{i}q_z)|^2$, where $\alpha = e^2\sqrt{\mu/(2\Omega_{\mathrm{LO}})}(\kappa_\infty^{-1} - \kappa_0^{-1})$, κ_∞ is the optical dielectric constant and Ω_{LO} is the LO phonon frequency. The form factor $|I(\mathrm{i}q_z)|^2 = \pi^2\sin^2 y/[y^2(y^2-\pi^2)^2]$, where $y = q_z a/2$. $N_{qq_z\lambda} = 1/[\exp(\Omega_{qq_z\lambda}/k_{\mathrm{B}}T) - 1]$ is the Bose distribution of phonon mode λ at temperature T. The second term inside the braces on the rhs of equation (A.1) results from the electron–impurity scattering under the random phase approximation, with N_{i} denoting the impurity concentration. $U_q^2 = \sum_{q_z}\{4\pi Z_{\mathrm{i}}e^2/[\kappa_0(q^2+q_z^2)]\}^2|I(\mathrm{i}q_z)|^2$ is the electron–impurity interaction matrix element, where Z_{i} represents the charge number of the impurity. Z_{i} is assumed to be 1 throughout our calculation. The third term is the contribution of the Coulomb interaction. Similarly, the scattering parts of the spin coherence are given by

$$\begin{aligned}\left.\frac{\partial\rho_{\boldsymbol{k}}}{\partial t}\right|_{\mathrm{scatt}} = \Bigg\{&\pi\sum_{qq_z\lambda} g^2_{qq_z\lambda}\delta(\varepsilon_{\boldsymbol{k}} - \varepsilon_{\boldsymbol{k}-\boldsymbol{q}} - \Omega_{qq_z\lambda})[\rho_{\boldsymbol{k}-\boldsymbol{q}}(f_{\boldsymbol{k}\frac{1}{2}} + f_{\boldsymbol{k}-\frac{1}{2}}) + (f_{\boldsymbol{k}-\boldsymbol{q}\frac{1}{2}} + f_{\boldsymbol{k}-\boldsymbol{q}-\frac{1}{2}} - 2)\rho_{\boldsymbol{k}}\\
&- 2N_{qq_z\lambda}(\rho_{\boldsymbol{k}} - \rho_{\boldsymbol{k}-\boldsymbol{q}})] + \pi N s_{\mathrm{i}}\sum_{\boldsymbol{q}} U_q^2\delta(\varepsilon_{\boldsymbol{k}} - \varepsilon_{\boldsymbol{k}-\boldsymbol{q}})[(f_{\boldsymbol{k}\frac{1}{2}} + f_{\boldsymbol{k}-\frac{1}{2}})\rho_{\boldsymbol{k}-\boldsymbol{q}}\\
&- (2 - f_{\boldsymbol{k}-\boldsymbol{q}\frac{1}{2}} - f_{\boldsymbol{k}-\boldsymbol{q}-\frac{1}{2}})\rho_{\boldsymbol{k}}] - \sum_{\boldsymbol{q}\boldsymbol{k}'}\pi V_q^2\delta(\varepsilon_{\boldsymbol{k}-\boldsymbol{q}} - \varepsilon_{\boldsymbol{k}} + \varepsilon_{\boldsymbol{k}'} - \varepsilon_{\boldsymbol{k}'-\boldsymbol{q}})\\
&\times\Big((f_{\boldsymbol{k}-\boldsymbol{q}\frac{1}{2}}\rho_{\boldsymbol{k}} + \rho_{\boldsymbol{k}-\boldsymbol{q}}f_{\boldsymbol{k}-\frac{1}{2}})(f_{\boldsymbol{k}'\frac{1}{2}} - f_{\boldsymbol{k}'-\boldsymbol{q}\frac{1}{2}} + f_{\boldsymbol{k}'-\frac{1}{2}} - f_{\boldsymbol{k}'-\boldsymbol{q}-\frac{1}{2}})\\
&+ \rho_{\boldsymbol{k}}[(1 - f_{\boldsymbol{k}'\frac{1}{2}})f_{\boldsymbol{k}-\boldsymbol{q}\frac{1}{2}} + (1 - f_{\boldsymbol{k}'-\frac{1}{2}})f_{\boldsymbol{k}-\boldsymbol{q}-\frac{1}{2}} - 2\,\mathrm{Re}(\rho^*_{\boldsymbol{k}'}\rho_{\boldsymbol{k}-\boldsymbol{q}})]\\
&- \rho_{\boldsymbol{k}-\boldsymbol{q}}[f_{\boldsymbol{k}'\frac{1}{2}}(1 - f_{\boldsymbol{k}'-\boldsymbol{q}\frac{1}{2}}) + (1 - f_{\boldsymbol{k}'-\frac{1}{2}})f_{\boldsymbol{k}'-\boldsymbol{q}-\frac{1}{2}} - 2\,\mathrm{Re}(\rho^*_{\boldsymbol{k}'}\rho_{\boldsymbol{k}'-\boldsymbol{q}})]\Big)\Bigg\}\\
&- \{\boldsymbol{k}\leftrightarrow\boldsymbol{k}-\boldsymbol{q}, \boldsymbol{k}'\leftrightarrow\boldsymbol{k}'-\boldsymbol{q}\}.\end{aligned} \tag{A.2}$$

References

[1] Ziese M and Thornton M J 2001 *Spin Electronics* (Berlin: Springer)
[2] Wolf S A *et al* 2001 *Science* **294** 1488
[3] Awschalom D D, Samarth N and Loss D 2002 *Semiconductor Spintronics and Quantum Computation* (Berlin: Springer)
[4] Damen T C *et al* 1991 *Phys. Rev. Lett.* **67** 3432
[5] Wagner J *et al* 1993 *Phys. Rev.* B **47** 4786
[6] Baumberg J J *et al* 1994 *Phys. Rev. Lett.* **72** 717
[7] Baumberg J J *et al* 1994 *Phys. Rev.* B **50** 7689
[8] Heberle A P, Rühle W W and Ploog K 1994 *Phys. Rev. Lett.* **72** 3887
[9] Buss C, Frey R, Flyizanis C and Cibert J 1995 *Solid State Commun.* **94** 543
[10] Crooker S A *et al* 1996 *Phys. Rev. Lett.* **77** 2814
[11] Crooker S A *et al* 1996 *Phys. Rev.* B **56** 7574
[12] Buss C *et al* 1997 *Phys. Rev. Lett.* **78** 4123
[13] Kikkawa J M, Smorchkova I P, Samarth N and Awschalom D D 1997 *Science* **277** 1284
[14] Kikkawa J M and Awschalom D D 1998 *Nature* **397** 139
[15] Kikkawa J M and Awschalom D D 1998 *Phys. Rev. Lett.* **80** 4313
[16] Ohno H 1998 *Science* **281** 951
[17] Ohno Y *et al* 1999 *Phys. Rev. Lett.* **83** 4196
[18] Meier F and Zakharchenya B P (ed) 1984 *Optical Orientation* (Amsterdam: North-Holland)
[19] Aronov A G, Pikus G E and Titkov A N 1983 *Zh. Eksp. Teor. Fiz.* **84** 1170 (Engl. transl. 1983 *Sov. Phys.–JETP* **57** 680)
[20] Fabian J and Sarma S D 1999 *J. Vac. Sci. Technol.* B **17** 1708
[21] Yafet Y 1952 *Phys. Rev.* **85** 478

[22] Elliot R J 1954 *Phys. Rev.* **96** 266
[23] D'yakonov M I and Perel' V I 1971 *Zh. Eksp. Teor. Fiz.* **60** 1954 (Engl. transl. 1971 *Sov. Phys.–JETP* **33** 1053)
[24] Bir G L, Aronov A G and Pikus G E 1975 *Zh. Eksp. Teor. Fiz.* **69** 1382 (Engl. transl. 1975 *Sov. Phys.–JETP* **42** 705)
[25] Wu M W and Ning C Z 2000 *Phys. Status Solidi* b **222** 523
[26] Wu M W and Kuwata-Gonokami M 2002 *Solid State Commun.* **121** 509
[27] Wu M W 2001 *J. Phys. Soc. Japan* **70** 2195
[28] Wu M W and Ning C Z 2000 *Eur. Phys. J.* B **18** 373
[29] Wu M W 2001 *J. Supercond.: Incorping Novel Mechanism* **14** 245 (*Preprint* cond-mat/0109258)
[30] Bronold F X, Martin I, Saxena A and Smith D L 2002 *Phys. Rev.* B **66** 233206
[31] Weng M Q and Wu M W 2002 *Phys. Rev.* B **66** 235109
[32] Weng M Q and Wu M W 2003 *J. Appl. Phys.* **93** 410
[33] Weng M Q and Wu M W 2003 *Phys. Rev.* B **68** at press
[34] Weng M Q and Wu M W 2003 *Phys. Status Solidi* b at press
[35] Wu M W and Metiu H 2000 *Phys. Rev.* B **61** 2945
[36] Dresselhaus G 1955 *Phys. Rev.* **100** 580
[37] Bychkov Y A and Rashba E 1984 *J. Phys. C: Solid State Phys.* **17** 6039
[38] Bychkov Y A and Rashba E 1984 *Sov. Phys.–JETP Lett.* **39** 78
[39] Lommer G, Malcher F and Rössler U 1988 *Phys. Rev. Lett.* **60** 728
[40] Haug H and Jauho A P 1996 *Quantum Kinetics in Transport and Optics of Semiconductors* (Berlin: Springer)
[41] Mahan G D 1981 *Many-Particle Physics* (New York: Plenum)
[42] Kuhn T and Rossi F 1992 *Phys. Rev. Lett.* **69** 977
[43] Slichter C P 1990 *Principles of Magnetic Resonance* 3rd edn (Berlin: Springer)
[44] Madelung O, Schultz M and Weiss H (ed) 1982 *Numerical Data and Functional Relationships in Science and Technology (Landolt–Börnstein New Series vol 17)* (Berlin: Springer)
[45] Averkiev N S, Golub L E and Willander M 2002 *J. Phys.: Condens. Matter* **14** R271
[46] Dyakonov M I and Kachorovskii V Y 1986 *Fiz. Tekh. Poluprov.* **20** 178 (Engl. transl. 1986 *Sov. Phys.–Semicond.* **20** 110)
[47] Lau W H, Oleberg J T and Flatté M E 2001 *Phys. Rev.* B **64** 161301